

# The chemical composition of a mild barium star HD202109 \*

Alexander V. Yushchenko<sup>1</sup>, Vera F. Gopka<sup>1,5</sup>, Chulhee Kim<sup>2</sup>, Yanchun Liang<sup>7,8,9</sup>, Faig A. Musaev<sup>3,4,6</sup>, and Gazinur A. Galazutdinov<sup>3,6</sup>

<sup>1</sup> Odessa Astronomical observatory, Odessa National University, Park Shevchenko, Odessa, 65014, Ukraine e-mail: [yua@odessa.net](mailto:yua@odessa.net), [gopka@arctur.tenet.odessa.ua](mailto:gopka@arctur.tenet.odessa.ua)

<sup>2</sup> Department of Earth Science Education, Chonbuk National University, Chonju 561-756, Korea, e-mail: [chkim@astro.chonbuk.ac.kr](mailto:chkim@astro.chonbuk.ac.kr)

<sup>3</sup> The International Centre for Astronomical, Medical and Ecological Research of the Russian Academy of Sciences and the National Academy of Sciences of Ukraine, Golosiiv, Kiev, 03680, Ukraine (ICAMER) e-mail: [zamt@burbonz.nalnet.ru](mailto:zamt@burbonz.nalnet.ru)

<sup>4</sup> Special Astrophysical observatory of the Russian Academy of Sciences, Nizhniy Arkhyz, Zelenchuk, Karachaev-Cherkesiya, 369167, Russia e-mail: [faig@sao.ru](mailto:faig@sao.ru), [gala@sao.ru](mailto:gala@sao.ru)

<sup>5</sup> Isaac Newton Institute, Santiago, Chile, Odessa branch, Ukraine

<sup>6</sup> Isaac Newton Institute, Santiago, Chile, SAO branch, Russia

<sup>7</sup> National Astronomical Observatories, Chinese Academy of Sciences, 100012, Beijing, P. R. China

<sup>8</sup> GEPI, Observatoire de Paris-Meudon, 92195 Meudon, France

<sup>9</sup> Institut für Astronomie und Astrophysik der Universität München, Universitäts-Sternwarte München, Scheinerstr. 1, 81679 München, Germany

Received Febrary XX, 2003; accepted Xxxxx XX, 2003

**Abstract.** We present the result of chemical abundances of a mild barium star HD202109 ( $\zeta$  Cyg) determined from the analysis of spectrum obtained by using a 2-m telescope at the Peak Terskol Observatory and a high-resolution spectrometer with  $R = 80,000$ , signal to noise ratio  $>100$ . We also present the atmospheric parameters of the star determined by using various methods including iron-line abundance analysis. For line identifications, we use whole-range synthetic spectra computed by using the Kurucz database and the latest lists of spectral lines. Among the determined abundances of 51 elements, those of P, S, K, Cu, Zn, Ge, Rb, Sr, Nb, Mo, Ru, Rh, Pd, In, Sm, Gd, Tb, Dy, Er, Tm, Hf, Os, Ir, Pt, Tl, and Pb have not been previously known. Under the assumption that the overabundance pattern of Ba stars is due to wind-accretion process, adding information of more element abundances enables one to show that the heavy element overabundances of HD202109 can be explained with the wind accretion scenario model.

**Key words.** Line: identification – Stars: abundances – Stars: atmospheres – Stars: evolution – Stars: chemically peculiar – Stars: binaries – Stars: individual: HD202109

## 1. Introduction

Barium stars were first categorized by Bidelman & Keenan (1951). Burbidge & Burbidge (1957) obtained the first quantitative result about the chemical composition of one of barium stars (HD46407) and reported overabundance of heavy elements. Burbidge et al. (1957) interpreted the overabundance in terms of the *s*-process. Another important finding in understanding the physical process of the formation of barium stars was the fact that these stars

are members of binary systems (McClure et al. 1980). A review of the developments of the theory of elements creation in stars was made by Wallerstein et al. (1997).

To explain the process of stellar evolution from abundance analysis, it is essential to construct detailed observed abundance patterns based on abundances of a large number of elements. Unfortunately, detailed abundance patterns are known only for limited number of stars including the Sun, for which abundances of 73 chemical elements are known (Grevesse & Sauval 1998). Some other stars with best-determined abundance patterns include GS22892-05 (abundance pattern based on 57 elements; Sneden et al. 2003), GS31082-001 (based on 38 elements with  $Z > 38$ ; Aoki et al. 2003; Sneden et al. 2000), Procyon (based on 55 elements; Yushchenko & Gopka 1996a,b),

Send offprint requests to: A.V. Yushchenko

\* Based on observations obtained at 2 meter telescope of Peak Terskol observatory near Elbrus Mountain, Northern Caucasus, Russia – International Center for Astronomical, Medical and Ecological Research (ICAMER), Ukraine & Russia

Przybylski's star (based on 54 elements; Cowley et al. 2000), and  $\chi$  Lupi (based on 51 elements; Leckrone et al. 1999).

Theoretical abundance patterns of *s*-process elements in barium stars was published, for example, by Cowley & Downs (1980), Malaney (1987), Liang et al. (2000). The most widely-accepted hypothesis about the element creation in barium stars is that the overabundances of heavy elements in the atmospheres of barium stars were produced by the accretion of matter ejected from their former AGB companions. These AGB companions have quickly evolved to be white dwarfs and can not be easily detected now.

In this paper, we attempt to construct the detailed abundance pattern of one of the barium stars by determining abundances of as many elements as possible, paying special attention to *s*-process elements. We tried to use high resolution observations in blue spectral region, to use the latest atomic data and the most updated spectrum synthesis method for better line identifications.

The star selected for our investigation is HD202109 ( $\zeta$  Cyg, BS 8115, 64 Cyg), which is a prototype mild barium star. The star was first noticed as a barium star by Bidelman. The first quantitative abundance analysis for this star was done by Chromey et al. (1969). Keenan & MacNeil (1976) determined the star's spectral class as G8+III-IIIa Ba 0.6. Griffin & Keenan (1992) reclassified the spectral class as G8+IIIa Ba 0.6 and published the orbit of the bright component of this spectroscopic binary. Griffin (1996) pointed out that the orbital period of the system ( $\sim 18$  years) is the longest among the the systems with moderate enhancement of *s*-process elements. Pourbaix & Jorissen (2000) investigated the HIPPARCOS transit data of HD202109, but long period did not permit them to find reliable orbit. The white dwarf companion was directly imaged from recent HST observations in UV filter by Barstow et al. (2001).

The previous works on the chemical composition of the star include those of Sneden et al. (1981), Gratton (1985), Berdyugina (1993) – CNO elements, Zacs (1994), and Boyarchuk et al. (2001) – heavier elements. Cohen et al. (1999) and Garett et al. (2001) used HD202109 as a comparison star and published the abundances of several elements.

We select HD202109 as our target for the following reasons. First, since chemical abundances are known for some elements from previous works, comparison to the previous results allows us to draw more reliable results. Second, the star is bright enough for us to acquire high-quality spectra by using a mid-size telescope. Third, HD202109 is an ideal target to test whether the accretion hypothesis can be applicable to barium stars with moderate enhancement of *s*-process elements, which is expected for barium stars with slow orbital motions. Fourth, since the star was observed in a wide range of wavelength spanning from X-ray to radio, it is possible to draw more concrete conclusions about the nature of this binary system.

## 2. Observations and data reduction

High resolution spectrum of HD202109 was obtained on September 19 in 2000 by using a coude-echelle spectrometer (Musaev et al. 1999) mounted on the 2-m "Zeiss" telescope at the Peak Terskol Observatory located near Elbrus mountain (Northern Caucasus) in Russia. The elevation of the observatory is 3,124 m above sea level.

We used one of middle resolution modes of the spectrograph with a resolving power of  $R = 80,000$ . The observed wavelength range,  $\lambda\lambda 3495 - 10000 \text{ \AA}$ , was covered by 85 echelle orders. In the observed spectrum, there are gaps between orders in the wavelength region of  $\lambda \geq 3780 \text{ \AA}$  and the width of each gap increases from  $0.5 \text{ \AA}$  to  $125 \text{ \AA}$  as the wavelength increases. The CCD, made by Wright Instruments, has a  $1,242 \times 1,152$  format and each pixel has a physical size of  $22 \mu\text{m}$ . The signal-to-noise ratio of the spectrum is not less than 100 over the whole wavelength range and reaches 300 or more in the blue and red parts of the spectrum.

First-stage data processing (background subtraction, echelle vector extraction from the echelle-images, and wavelength calibration) is conducted by using the latest version of PC-based DECH software (Galazutdinov 1992). For other processes including continuum placement, we use URAN software developed by one of us (Yushchenko 1998). Continuum placement was made taking into account the calculated spectrum. More details about this type of continuum placement procedure were discussed for example by Walgren (1995).

## 3. Atmospheric parameters

With the processed data, we then determine the atmospheric parameters including the effective temperature,  $T_{\text{eff}}$ , surface gravity,  $\log g$ , microturbulence velocity,  $v_{\text{micro}}$ .

### 3.1. Effective temperature from colors

We first determine  $T_{\text{eff}}$  of HD202109 from color information. For this, we use two colors of  $V - K$  and  $b - y$ . Following the calibrations of Di Benedetto (1998) for  $V - K$  and Alonso et al. (1999) for  $b - y$ , we find that the temperatures determined from these two colors are  $T_{\text{eff}} = 4927 \text{ K}$  and  $4903 \text{ K}$ , respectively.

We compare our results of  $T_{\text{eff}}$  with previous determinations based on different methods and data. Andrievsky et al. (2002) determined  $T_{\text{eff}}$  of the star by using different photometric data and calibrations. They found five values of  $T_{\text{eff}} = 5130 \text{ K}, 5070 \text{ K}, 4900 \text{ K}, 5120 \text{ K}$ , and  $5100 \text{ K}$  and presented  $T_{\text{eff}} = 5100 \text{ K}$  as a representative value. Gray & Brown (2001) used the line-ratio method, and found the value  $T_{\text{eff}} = 4987 \text{ K}$ . It should be noted, that Gray & Brown (2001) used HD202109 as one of the calibrating stars to set their temperature scale. Upon our request, V. Kovtyukh kindly provided his determination based on similar methodic - depth ratios of iron lines. By

using the latest version of Kovtyukh & Gorlova (2000) methodic, he found  $T_{eff} = 5044 \pm 44$  K.

For the effective temperature, one may use the temperature determined from color information, but we decide to choose the value determined from the iron-line abundance analysis because it is known that the precision of  $T_{eff}$  determined from spectroscopic determinations is significantly higher than that of the temperature determined from color information (Boyarchuk 2001).

### 3.2. Atmospheric parameters from iron line abundance analysis

In the usual process, atmospheric parameters from iron line analysis are determined by investigating the correlation(s) between the observed equivalent widths,  $\log(W_{\lambda}/\lambda)$ , (and the excitation potential,  $E_{low}$ ) of iron lines and the iron abundances calculated based on the equivalent widths of the individual lines by assuming a certain atmosphere model. In this process, it is customary to use fixed values of  $T_{eff}$  and  $\log g$ , under the assumption that these parameters can be constrained from other informations (for example from colors), and leave  $v_{micro}$  as the only free parameter. Variation of this parameter permit to avoid the influence of the possible uncertainties in effective temperature and surface gravity.

Yushchenko et al. (1999) noticed that the scattering information of the iron abundances derived from different iron lines is useful in determining correct atmospheric parameters. The scattering for models with false parameters are usually larger than for models with true parameters.

In our analysis, we, therefore, determine the atmospheric parameters not only by leaving all of them as free parameters but also by using additional information of scattering in the derived iron abundances.

For atmospheric parameter determinations, we select 89 clean Fe I lines in the synthetic spectrum of HD202109 and measure their equivalent widths in observed spectrum by modelling their profiles as gaussian.

For the oscillator strengths of the individual iron lines, we use the solar determinations of Gurtovenko & Kostik (1989). For lines where oscillator strengths are not available in Gurtovenko & Kostik (1989), we use solar values computed by using the spectrum synthesis method. Details about the line selection and the synthetic spectrum calculations are described in § 4. Once oscillator strengths are set, the iron abundances are derived from the individual lines by using WIDTH9 code of Kurucz (1995).

To fully characterize general binary systems, it is required to determine two sets of atmospheric parameters for the individual component stars and the flux ratio between them. We note, however, that although HD202109 is a binary, the flux from the white dwarf can be neglected in the used wavelength interval. For atmospheric parameter determinations of a binary where the fluxes of the component stars are of the same order, see Yushchenko et al. (1999).

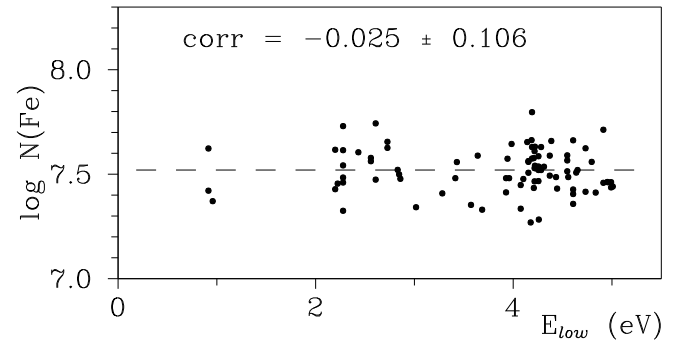


**Fig. 1.** The correlation between the iron abundances determined from 89 Fe I lines in the spectrum of HD202109 and the excitation energies,  $E_{low}$ , of the individual lines. Our final atmosphere parameters and abundances of other chemical elements were used.

For atmosphere models, we use Kurucz (1995) data base. We make  $21 \times 6$  subgrid of atmosphere models by subdividing the grid of Kurucz data base. The ranges (and intervals) of the individual parameters are  $4750 \text{ K} \leq T_{eff} \leq 5250 \text{ K}$  ( $\Delta T_{eff} = 25 \text{ K}$ ) for the effective temperature and  $2.5 \leq \log g \leq 3.0$  ( $\Delta \log g = 0.1$ ) for the surface gravity. Calculations for all models were made with 41 values of microturbulent velocity  $1.0 \text{ km s}^{-1} \leq v_{micro} \leq 3.0 \text{ km s}^{-1}$  ( $\Delta v_{micro} = 0.05 \text{ km s}^{-1}$ )

Based on each set of atmosphere parameters, we compute iron abundances corresponding to the individual lines. For iron abundances computed for each set of atmosphere parameters, we then calculate the scattering of the abundances and the coefficient(s) of the correlation(s) between the equivalent widths (and the excitation potentials) and the iron abundances.

Among the tested models, the best atmosphere model is chosen as the one providing zero (or very close to zero) correlation coefficients and minimal scattering in the derived iron abundances. We find that the best model has atmosphere parameters of  $T_{eff} = 5050 \text{ K}$ ,  $\log g = 2.8$ , and  $v_{micro} = 1.45 \text{ km s}^{-1}$ . We note that our determination of  $T_{eff}$  is very close to the value of Kovtyukh determined by using the line-depth ratio method. We present the correlation between  $\log N(\text{Fe})$  and  $\log(W_{\lambda}/\lambda)$  in Figure 1 and the correlation between  $\log N(\text{Fe})$  and  $E_{low}$  in Figure 2 for the best atmosphere model. In Table 1, we compare our results of atmospheric parameters with those of other determinations.

It is noteworthy that since our method uses scattering information of iron abundances, the method enables us to determine the iron abundance. We found that the iron abundance of HD202109 is  $+0.01 \pm 0.11$  dex relative to the solar value.

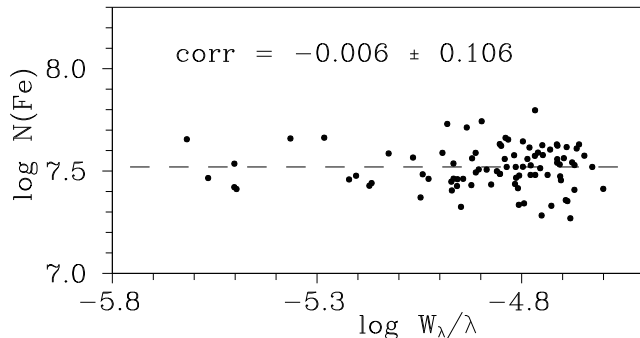


**Fig. 2.** The correlation between the iron abundances determined from 89 Fe I lines in the spectrum of HD202109 and the equivalent widths,  $\log(W_\lambda/\lambda)$ , of the individual lines.

**Table 1.** Atmospheric parameters of HD202109 ( $\zeta$  Cyg)

reference	$T_{eff}$ (K)	$\log g$	$v_{micro}$ (km s $^{-1}$ )
Chromey (1969)	5143		
Pilachowski (1977)	4893	2.8	
Sneden et al. (1981)	4870	2.5	2.0
	5000	2.8	2.2
Gratton et al. (1982)	4941	2.0	
Gratton (1985)	4950	2.0	2.4
Fernandez-Villacanas et al. (1990)	4900	2.0	
McWilliam (1990)	4990	2.87	
Berdugina (1993)	5000	2.7	2.0
Berdugina & Savanov (1994)	5000	2.8	
Zacs (1994)	5050	2.8	3.5
Cohen et al. (1999)	4950	2.7	1.6
Boyarchuk et al. (2001)	4977	2.52	1.4
Gray & Brown (2001)	4987		
Andrievsky et al. (2002)	5100	2.5	1.5
This paper	5050	2.8	1.45

## 4. Abundance Analysis

### 4.1. Synthetic Spectrum

We determine the abundances of elements except iron by using the synthetic spectrum method. In order to construct accurate synthetic spectra, it is necessary to find the parameters of line broadening.

The magnetic field of HD202109 were investigated by Tarasova (2002). She found the values  $-5.4 \pm 0.2$ ,  $-0.4 \pm 2.0$  and  $0.2 \pm 1.8$  gauss. The field of this strength can not influence significantly on our final results. Rotation velocity of HD202109 can be not negligible:  $v_{rot} = 3.4 \pm 0.5$  km s $^{-1}$  determined by Gray (1989) and  $v_{rot} \lesssim 1.0$  km s $^{-1}$  determined by de Medeiros & Mayor (1999).

We assume that lines are broadened mainly by the macroturbulence velocity. We estimate the macroturbulent velocity by analyzing the profiles of iron lines with precise oscillator strengths. We find that  $v_{macro} = 3.2 - 3.5$  km s $^{-1}$ . This value includes all possible mechanisms

of line broadening. Gaussian model of macroturbulence (Gray 1976) was used.

With the inputs of all these parameters, the synthetic spectra are constructed by using the SYNTHE code of Kurucz (1995). We used various lists of spectral lines. These include all atomic and molecular lines of Kurucz (1995) database, Morton (2000) lines, DREAM database (Biemont et al. 2002) lines for lanthanides and actinides, part of the lines from VALD database (Piskunov et al. 1995), and lines in other lists. We take into account the hyperfine-structure lines and isotopic splitting of the lines for Mn, Cu, and Eu. Split line data are taken from Kurucz (1995) database.

### 4.2. Line identifications

To better identify heavy element lines, the synthetic spectrum used for line identifications is produced by increasing the abundances of uninvestigated heavy elements by an amount of +0.5 dex compared to the solar system values.

For identification of lines of some element we selected all not strongly-blended lines of this element from the results of synthetic spectrum calculations and viewed these lines in the observed spectrum to select the best lines for abundance analysis. The observed and synthetic spectra of HD202109 and of the Sun were displayed simultaneously on the computer screen. It permits us to avoid errors in identifications and to increase the number of selected lines. URAN code of Yushchenko (1998) was used.

In Figures 3 and 4, we present the parts of the observed spectrum of HD202109 and its approximation by the synthetic one.

### 4.3. Abundance Determinations

Once the individual lines are identified, we then determine the abundances of elements. For line identifications and abundance determinations, we use the URAN code of Yushchenko (1998), in which abundances are computed in semiautomatic mode. For approximation of observed spectrum by synthetic one we changed the oscillator strengths of all lines in the uninvestigated region, except for the lines located closer than 0.03 Å to the investigated line. SYNTHE code of Kurucz (1995) was used for calculations of the synthetic spectra.

More descriptions about this type of codes for semiautomatic and automatic abundance analysis are found in Cowley (1995), Tsymbal & Cowley (2000) – MERSEN code, Valenty & Piskunov (1996) – SME, Erspamer & North (2002), and Bruntt et al. (2002). Although these codes use different algorithms, they allow one to significantly increase the list of investigated lines and minimize manual work.

As initial abundances for the computation of synthetic spectrum, we use the values published in earlier investigations. This permits us to include moderately blended lines for abundance analysis and thus maximize the number of

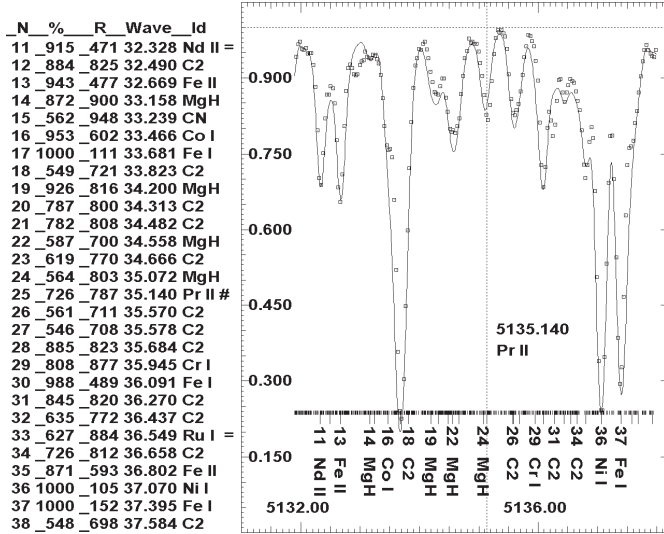


**Fig. 3.** The example of the spectrum of HD202109. The squares are observed spectrum. The solid line is the synthetic one. The position of the strong and faint lines in the synthetic spectrum are shown by long and short dashes in the bottom part of the figure. Part of the strong lines are marked by numbers and identification. In the left part of the figure we place a table with the result of calculations of synthetic spectrum. In this table the first column is the line number, the second column is the portion of this line in the total line absorption coefficient at the wavelength of the center of the line in the synthetic spectrum. For clean line the value in this column must be 1000. In the third column one can find the value of synthetic spectrum at the center of the line. The continuum value is 1000. Only strong line are listed. The values of synthetic spectrum in the table are not smoothed by instrumental and macroturbulence profiles. In the last two columns we show the last figures of the wavelengths of these lines and their identifications. Lines of *r*-, *s*-processes elements are marked by equal sign. Pr II  $\lambda$  5135.140 Å line is marked by # sign in the table and by vertical dashed line in the spectrum. This and the next figures are the PrintScreen output of URAN software (Yushchenko 1998).

elements with determined abundances. In addition, good guess of initial abundances can minimize the computation time by reducing the number of iterations in line-fitting process.

To compare the abundances of individual elements of HD202109 with those of the Sun, we also calculate the solar abundances for the investigated lines. For this calculation, we use Liege Solar atlas (Delbouille et al. 1974) and Holweger & Muller (1974) atmosphere model. The adopted values of the microturbulent and macroturbulent velocities are  $1.0 \text{ km s}^{-1}$  (Gopka & Yushchenko 1995) and  $1.8 \text{ km s}^{-1}$ , respectively. The continuum in the Liege Solar atlas is corrected in accordance with Arderberg & Virdeforce (1979) and Rutten & van der Zalm (1984). We use the same SYNTHE and URAN codes for synthetic

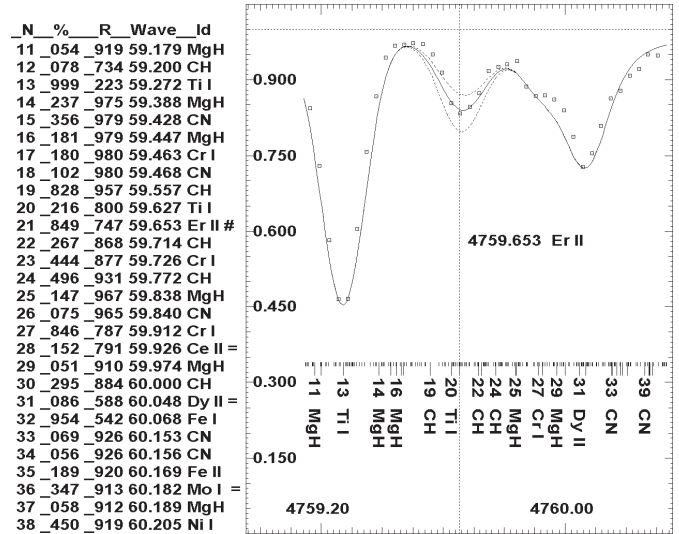


**Fig. 4.** Example of approximation of observed spectrum (squares) of HD202109 by calculated one. Solid line – spectrum, calculated with our final abundances. Dashed lines – spectra calculated with erbium abundances changed by  $\pm 0.2$  dex from the best value. The central line of the plot – Er II  $\lambda$  4759.653 Å is marked by # sign in the table and by vertical dashed line in the spectrum.

spectrum construction, line identifications, and abundance determinations.

We present the partial list of the determined abundances of elements derived from the individual lines of HD202109 in Table 2 (for iron lines) and 3 (for lines of other elements). Table 2 contains the element code (26.00 for Fe I), wavelength, equivalent width (Eq.W.), oscillator strength ( $\log gf$ ), excitation potential, derived abundances (expressed in the scale of  $\log N(H) = 12$ ). Table 3 contains element code, wavelength, oscillator strength, excitation potential, derived abundances for  $\zeta$  Cyg and for the Sun and the difference between these abundances ( $\Delta$ ). For lines without counterparts in the solar spectrum Grevesse, N., & Sauval (1998) solar system abundances were used. The electronic versions of the full lists can be obtained at the Web sites: “[users.odessa.net/~yua](http://users.odessa.net/~yua)” and “[yushchenko.netfirms.com](http://yushchenko.netfirms.com)”

In Tables 4 and 5, we present the final list of the abundances of 51 elements, which are computed by averaging the abundances derived from all lines of the individual elements. Table 4 contains CNO data obtained by Sneden et al. (1981), Gratton (1985), Berdyugina (1993), Cohen et al. (1999) and our result for oxygen.

The relative abundances of other elements (listed in Table 5) are compared with the determinations of Zacs (1994) and Boyarchuk et al. (2001). Our results (except iron) were obtained with spectrum synthesis method. Zacs (1994) and Boyarchuk et al. (2001) data were calculated with model atmospheres method. Elements with lines having no counterparts in the solar spectrum are marked by ‘\*’ sign. For these elements abundances are given with respect to the solar values (Grevesse & Sauval 1998) of

**Table 2.** Fe I and Fe II lines in the spectrum of HD202109 (example, full table is available in electronic form)

element code	$\lambda$ (Å)	Eq.W. (mÅ)	$\log gf$	$E_{low}$ (eV)	$\log N$
26.01	4620.52	85	-3.57	2.828	7.827
26.01	5197.58	114	-2.48	3.230	7.693
26.01	5234.63	115	-2.42	3.221	7.635
26.01	6369.46	43	-4.37	2.891	7.707
26.01	6432.68	71	-3.83	2.891	7.728
26.01	6456.38	85	-2.32	3.903	7.594

**Table 3.** Abundances of chemical elements calculated from individual lines in the spectrum of  $\zeta$  Cyg (HD202109) and in the solar spectrum (example, full table is available in electronic form)

element code	$\lambda$ (Å)	$\log gf$	$E_{low}$ (eV)	$\log N$	$\Delta$
				$\zeta$ Cyg	Sun
72.01	4093.155	-1.090	.452	1.01	.56
76.00	3528.598	-1.700	.000	1.46	1.41
76.00	3501.163	-.510	1.841	1.96	1.41
77.00	3515.947	-1.580	.881	< 1.75	
77.00	3594.388	-1.550	.881	< 1.85	
78.00	3638.789	-1.340	1.254	1.8	
81.00	3519.210	.141	.966	< 1.4	
82.00	3683.462	-.555	.969	< 2.1	
82.00	3639.567	-.715	.969	< 2.1	

the corresponding elements. Also listed are the numbers of lines, ( $n$ ), from which the mean abundances of the individual elements are computed. The uncertainty of each element's abundance is estimated by computing the standard deviation of the abundances derived from the individual lines of the element. The uncertainties are, therefore, presented only for elements whose abundances are determined based on more than two lines.

We investigated the abundances of 47 elements. The abundances of Li, C, N, and Ba are taken from the papers mentioned above. The total abundance sample consists of 51 elements. *s*-process elements show overabundances in the atmosphere of this star.

We note that the abundances of P, S, K, Cu, Zn, Ge, Rb, Sr, Nb, Mo, Ru, Rh, Pd, In, Sm, Gd, Tb, Dy, Er, Tm, Hf, Os, Ir, Pt, Tl, and Pb are determined for the first time in this paper.

#### 4.4. Uncertainties in abundances

The determined abundances of elements are subject to uncertainties caused by various sources. The uncertainties in the determined abundances caused by the uncertainty of the atmosphere model can be estimated by investigating how the iron abundance varies depending on the adopted values of atmospheric parameters. We find that the variations of the iron abundance caused by the small deviations of  $\Delta T_{eff} = 100$  K,  $\Delta v_{micro} = 0.1$  km s<sup>-1</sup>, and

**Table 4.** CNO abundances in the atmosphere of HD202109 with respect to their abundances in the solar atmosphere

	Sneden et al. (1981)	Gratton (1985)	Berdyugina (1993)	Cohen et al. (1999)	This work	$n$
C	-0.18	-0.10	-0.19			
N	+0.58	+0.61	+0.23			
O	+0.04	-0.34	+0.02	+0.35	-0.22:	1

$\Delta \log g = 0.2$  are 0.06 dex, 0.10 dex, and 0.01 dex, respectively.

Of course, the abundances of different species will have different dependencies on the perturbations in the atmosphere parameters. For example, we find that the carbon abundance estimated based on the atmosphere model adopted by Cohen et al. (1999) differs from our determination by an amount of 0.23 dex. We note, however, that our adopted atmospheric parameters of HD202109 agree well with other determinations and thus we believe that the uncertainty in the determined abundances due to the adopted atmosphere model is unlikely to be large.

If we adopt one of the parameters with some uncertainty, we try to select the other parameters to minimize correlation coefficients and scattering of the results. For example, the metallicity derived in our investigation is +0.01 dex, and if we adopt the parameters of Boyarchuk et al. (2001) it will be changed by 0.04 dex only.

## 5. Observed abundance pattern

### 5.1. CNO elements

From Table 4, one finds that the abundances of these elements show considerable differences from one determination to another. In our analysis, we determine the abundance of only oxygen. We investigate the cause of the differences, focusing mainly on the difference between the oxygen abundances determined by us and Cohen et al. (1999), for which the difference is the greatest. We find several possible causes of differences.

First, both analyses are based on different oxygen lines. Our oxygen abundance is derived from line  $\lambda 6300.304$  Å. On the other hand, the oxygen abundance determined by Cohen et al. (1999) was based on triplet  $\lambda\lambda 7771-7775$  Å. Since this triplet is located at a gap in our spectra, we could not use it for abundance analysis.

Second, the lines used for both analyses are affected by blending. The  $\lambda 6300.304$  Å line used for our analysis is contaminated by Ni line. Among the three lines used for Cohen et al.'s analyses, only the  $\lambda 7771.944$  Å line is free from blending and the other two lines are contaminated by CN lines. The abundance of oxygen, calculated with Cohen et al. (1999) value of equivalent width of line  $\lambda 7771.944$  Å and with our parameters are greater than the value calculated using spectrum synthesis (with our parameters) for  $\lambda 6300.304$  Å line only by 0.09 dex.

**Table 5.** The abundances of chemical elements (except CNO) in the atmosphere of HD202109 with respect to the abundances in the solar atmosphere.

element	[N/N <sub>H</sub> ] (n)			element	[N/N <sub>H</sub> ] (n)		
	Zacs (1994)	Boyarch- uk et al. (2001)	This work		Zacs (1994)	Boyarch- uk et al. (2001)	This work
3 Li I	-0.14	(1)		39 Y I	+0.37±.24 (3)	+0.30	+0.15±.15 (3)
8 O I			-0.22: (1)	Y II			+0.48±.16 (22)
11 Na I	-0.35	(2)	+0.19	+0.24±.08 (4)	40 Zr I	-0.08±.20 (5)	+0.21±.06 (10)
12 Mg I	-0.51	(2)		Zr II			+0.52±.18 (12)
13 Al I			+0.16	+0.12±.12 (8)	41 Nb II*		+0.43 (1)
14 Si I	+0.14±.13 (3)	+0.09		42 Mo I			+0.20 (2)
Si II			+0.26 (2)	44 Ru I*			+0.32±.08 (3)
15 P I			+0.10 (1)	45 Rh I*			<+0.2 (2)
16 S I			+0.00±.12 (3)	46 Pd I*			+0.32: (1)
19 K I			-0.17 (2)	49 In I			+0.11: (1)
20 Ca I	+0.08±.19 (4)	-0.03	+0.02±.09 (5)	56 Ba II	+0.41±.13 (3)	+0.54	
21 Sc I	+0.04±.30 (4)	-0.02	+0.06±.11 (4)	57 La II	+0.38±.15 (3)	+0.45	+0.51±.20 (12)
Sc II			+0.08±.15 (10)	58 Ce II	+0.55 (1)	+0.33	+0.37±.18 (45)
22 Ti I	-0.17±.22 (21)	-0.11	-0.20±.17 (70)	59 Pr II	+0.32±.13 (3)	+0.43	+0.19±.19 (6)
Ti II			-0.03±.13 (30)	60 Nd II		+0.23	+0.42±.17 (70)
23 V I	-0.13±.18 (16)	-0.04	-0.03±.14 (41)	62 Sm II			+0.34±.18 (15)
V II			+0.17 (1)	63 Eu II	-0.05 (2)	+0.22	+0.32±.12 (3)
24 Cr I	-0.06±.18 (11)	-0.08	-0.17±.13 (65)	64 Gb II			+0.27±.19 (4)
Cr II			+0.10±.10 (15)	65 Tb II*			+0.1 (1)
25 Mn I	-0.30±.13 (5)		-0.25±.17 (21)	66 Dy II			+0.33±.18 (4)
26 Fe I	+0.12±.23 (51)	-0.03	+0.01±.11 (89)	68 Er II			+0.35 (1)
Fe II			+0.06±.07 (6)	69 Tm II			<+0.2 (1)
27 Co I	-0.22±.12 (6)	-0.13	+0.07±.11 (28)	72 Hf II*			+0.45: (1)
28 Ni I	-0.05±.25 (10)	-0.09	-0.09±.17 (74)	76 Os I*			+0.30: (2)
29 Cu I			-0.01 (1)	77 Ir I*			<+0.4 (2)
30 Zn I			-0.08±.09 (4)	78 Pt I*			+0.0 (1)
32 Ge I			+0.08 (1)	81 Tl I*			<+0.5 (1)
37 Rb I*			-0.07 (1)	82 Pb I*			<+0.2 (2)
38 Sr I			+0.26 (2)				

Third, the difference between the adopted atmosphere models also have some influence on the determined oxygen abundances. We recompute the oxygen abundance from  $\lambda 6300.304 \text{ \AA}$  line based on the atmosphere model adopted by Cohen et al. (1999) and find that it is higher than our original oxygen abundance by an amount of 0.23 dex.

CNO abundances are important in the abundance determinations of other elements. We calculated several synthetic spectra for the whole observed region with our parameters of atmosphere model and different CNO abundances. We choose to use the values of Gratton (1985), which produce a synthetic spectrum matching the observed spectra best among the determinations listed in Table 4.

## 5.2. Na to K

Our results for these elements are close to Boyarchuk et al. (2001) data for common elements. On the other hand, our values show some differences from the data of Andrievsky et al. (2002), which were released just after we completed the major part of our abundance determinations. For example, the NLTE value of the sodium abundance deter-

mined by Andrievsky et al. (2000) is +0.35 dex compared to our value of +0.24 dex. We suspect that the differences may be caused by their adoption of NLTE atmosphere model.

Our result of Mg abundance is in a good agreement with that of Cohen et al. (1999). Although the abundances of Si determined by Boyarchuk et al. (2001) and Cohen et al. (1999) are slightly higher than our value, all these values including ours are consistent with the solar abundance in the range of errors. Our results for P, S, and K indicate that the abundances of these elements are close to the solar values.

## 5.3. Ca to Ni

These elements produce majority of lines in the spectra of normal stars. We find that our value of iron abundance, +0.01 dex, agrees well with most previous determinations, ranging -0.17 to +0.10 dex (Cayrel de Strobel et al. 1997) except the value of Andrievsky et al. (2002), +0.15 dex. We suspect that the higher value of Andrievsky et al. (2002) is caused by the use of narrow wavelength-range

spectra in their abundance analysis. Because of this reason their [Na/Fe] for HD202109 can be higher.

We also find that the abundances derived from neutral and ionized lines result in similar values for Fe and Sc, while the values of Ti, V, and Cr show differences of  $\sim 0.2$  dex.

The abundance of Mn, which is estimated by using *hfs* data from Kurucz (1995) data base, indicates that this element is slightly underabundant.

For elements in this group, we find that the determined abundances show large fluctuation compared to the solar values. This fluctuation may be the intrinsic characteristic of the abundance patterns of HD202109 or caused by inadequate sophistication of atmosphere model.

#### 5.4. *r*-, *s*-process elements

For Y and Zr, we find inconsistencies between the abundances derived from neutral and ionized lines. Mean result for two ions of Y is in perfect agreement with Boyarchuk et al. (2001) and Zacs (1994).

For line identifications of lanthanides, we use both VALD line list (Piskunov et al. 1995) and DREAM (Biemont et al. 2002) data base. We expected that by using the DREAM data base we could identify more lanthanide lines based on the previous experience in the spectral analysis of Przybylski's star (Yushchenko et al. 2002). For HD202109, however, we could identify only a few more lines. We find that our results are consistent with Boyarchuk et al. (2001) and Zacs (1994) data for common elements.

From our investigation of the spectrum of HD202109, we are able to determine abundances of *r*-, *s*-process elements whose abundances were not previously known. These elements include Cu, Zn, Ge, Rb, Nb, Mo, Ru, Rh, Pd, In, Tb, Er, Tm, Hf, Os, Ir, Pt, Tl, and Pb. For most of these elements, we derive their abundances based on one or two lines and for some of these elements we can set only the upper limits. However, even these informations are very useful in constraining the parameters of the wind accretion model, which is described in the next section.

#### 6. Predicted heavy element abundances

As presented and shown in Table 5 and Figure 5, respectively, the determined abundances of neutron-capture (n-capture) process elements (hereafter heavy elements) of HD202109 are overabundant. Two peaks at  $Z \sim 39-40$  and  $Z \sim 56-57$  are obvious due to the neutron magic number 50 and 82 nuclei on the path of *s*-process nucleosynthesis occurred in the interiors of AGB stars.

Then the question is what causes the heavy element overabundances in barium stars? It is generally believed that the overabundances were caused by binary accretion, where Ba stars accreted the ejected material from their companions, formerly AGB stars and currently white

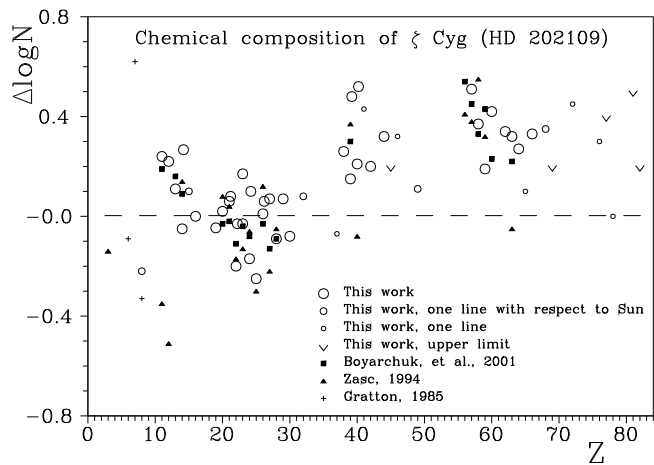


**Fig. 5.** The abundances of chemical elements and ions in the atmosphere of HD202109 with respect to their abundances in the solar atmosphere. Our data and data of Boyarchuk et al. (2001), Zacs (1994), and Gratton (1985) are shown for comparison.

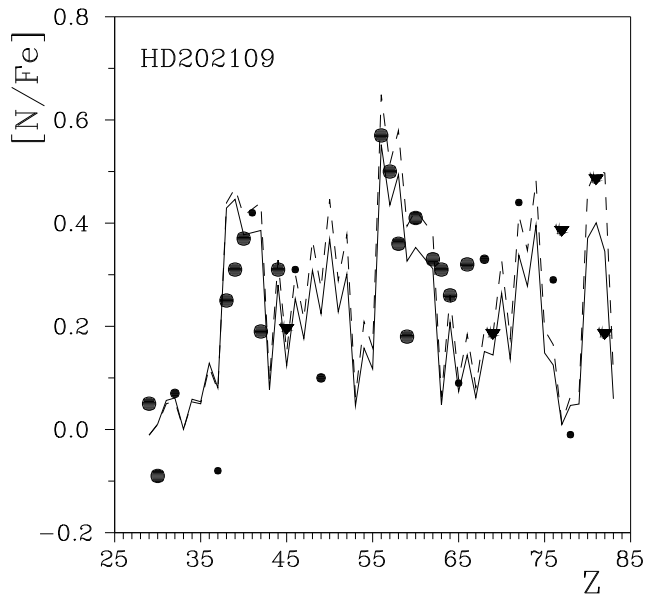


**Fig. 6.** The comparison of observed composition of heavy elements in the atmosphere of HD202109 with predicted abundances of these elements. Solid line – calculation with  $a=1.5$ , dashed line –  $a=1.8$ . Circles and triangles – observational data. For all elements except barium we plotted our results from Table 5, Boyarchuk et al. (2001) value was plotted for barium. Big circles – more than 1 line were measured for this element, middle circles – one line with respect to Sun, small circles – one line without direct comparison with the solar spectrum. Triangles – upper limit. For Y and Zr the weighted mean of abundances from the lines of first and second spectra are plotted.

dwarfs, which synthesized these heavy elements by themselves and ejected the elements into interstellar medium through stellar wind (Liang et al. 2000 and reference therein).

In the previous paper (Liang et al. 2000), the *s*-process nucleosynthesis of AGB star with mass  $3M_{\odot}$  and solar metallicity was calculated. At the same time, an angular momentum conservation model of wind accretion in binary systems was set up. Combining these two parts of work, the theoretical heavy-element abundances of barium stars were calculated, and the observed abundances of some sample barium stars were explained successfully.

In this section, we check whether the binary accretion model can also explain the heavy element overabundance of HD202109 by comparing the abundance pattern determined from our spectral analysis with the theoretical one calculated based on the model of Liang et al. (2000).

Following Liang et al. (2000), we compute the theoretical abundances of heavy elements in two steps. In the first step, we calculate the overabundances of the intrinsic AGB star at each ejection by adopting the theory of *s*-process nucleosynthesis and the latest TP-AGB model (Straniero et al. 1995; Straniero et al. 1997; Gallino et al. 1998; Busso et al. 1999). Then, the overabundances of heavy elements in the atmosphere of barium star are calculated by accreting the ejected matter predicted from the model of wind accretion and mixing them on successive occasions. For more details about the scenarios of *s*-process nucleosynthesis and the orbital evolution of the binary system, see Liang et al. (2000) and Liu et al. (2000).

The second step calculation needs main sequence mass of barium star. Thus, we estimated the mass of HD202109 by using the stellar evolution tracks given by Girardi et al. (2000). The derived mass from  $M_{\text{bol}}-\log T_{\text{eff}}$  diagram is  $\sim 3.05 M_{\odot}$ , which reveals that HD202109 is a mild barium star (Jorissen et al. 1998; Liang et al. 2003).

Therefore, the adopted wind accretion model is:  $3.0 M_{\odot}$  and  $2.5 M_{\odot}$  for the main-sequence masses of the intrinsic AGB star (the current white dwarf companion) and the barium star, respectively;  $v_{ej} = 15 \text{ km s}^{-1}$  for the wind velocity; and the accretion rate is 0.15 times of the Bondi-Hoyle's accretion rate (Liang et al. 2000).

In calculation, the resulted eccentricity of the orbit and orbital period of barium star system match the values of  $e = 0.22$  and  $P = 6489$  days, respectively, which are determined observationally by Griffin & Keenan (1992).

In Figure 6, the theoretical abundance pattern of HD202109 (the lines) and the pattern determined from our spectral analysis (the points) are presented. The two theoretical abundance pattern curves are corresponding to the neutron exposures of  $a = 1.5$  (solid curve) and  $1.8$  (dashed curve). “ $a$ ” refers the neutron exposure occurred in interior of its AGB star companion, and represents the times of the corresponding exposures in the  $^{13}\text{C}$  profile suggested by Gallino et al. (1998) (For more details, see Liang et al. 2000).

From Fig. 6, one finds that the calculated abundance pattern is consistent with the detailed pattern of the ob-

served abundances. That means that the heavy element overabundances of HD202109 may be resulted by accreting the ejecta of its AGB star companion through wind accretion. And the neutron exposure of the *s*-process nucleosynthesis occurred in the interior of the AGB companion corresponds to  $a = 1.5-1.8$ .

## 7. Conclusion

In this paper we tried to made the detailed analysis of abundances of *s*-process elements in the atmosphere of mild barium star HD202109.

The atmosphere parameters were found from the careful analysis of iron abundances, calculated from individual iron lines. Taking into account the increasing of scattering of the mean abundance in the case of using the wrong atmosphere parameters, we were able to develop the method of determination of effective temperature, surface gravity, microturbulent velocity and metallicity from the analysis of the lines of iron.

We used differential spectrum synthesis for calculation of the majority of investigated elements, taking the solar spectrum as a comparison one. The abundances of 47 elements in the atmosphere of HD202109 were found. We found the abundances of several elements near the last peak of the abundances of *s*-process elements in barium stars - the elements near atomic number  $Z=80$ . The abundances of Li, C, N, Ba were known from previous investigations of this star. The total abundance sample consists of 51 elements. It is the most detailed abundance pattern for barium stars.

We calculated the theoretical abundances of heavy elements of barium stars by using the AGB stars nucleosynthesis and the wind accretion model in barium binary systems. The observed abundances of as many heavy elements of HD202109 are consistent with the predicted abundances. It was shown that the barium star HD202109 can be formed through wind accretion scenario. The corresponding neutron exposure in the *s*-process nucleosynthesis occurred in the interior of its AGB star companion is  $a = 1.5$  to  $a = 1.8$ .

As the studies shown, the barium stars with orbital period  $P > 1600$  days can be formed through wind accretion (Liang et al. 2000; Liang et al. 2003). Jorissen et al. (1998) suggested the corresponding period is 1500 days. Possibly, the barium stars with lower orbital period form through other scenarios: dynamically stable late case C mass transfer or common envelope ejection. The studied star, HD202109 ( $P=6489$  days), provide strong support for this suggestion by the consistency between the observed abundances of as many heavy elements and the corresponding predicted abundances from our wind accretion model.

*Acknowledgements.* We would like to thank to L. Delbouille and G. Roland for sending us the Liege Solar Atlas, to C. Han and L. Zacs for helpful discussion about the work. We use data from NASA ADS, SIMBAD, CADC, VALD, NIST, and

DREAM databases and we thank to the teams and administrations of these projects. The paper was (partially) supported by research funds of Chonbuk National University, Korea.

## References

Alonco, A., Arribas, S., & Martinez-Roger, C. 1999, *A&AS*, 140, 261

Andrievsky, S.M., Egorova, I.A., Korotin, S.N., & Burnage, R. 2002, *A&A*, 389, 519

Aoki, W., Honda, S., Beers, T., & Sneden, C., 2003, *ApJ*, 586, 506

Arderberg, A., & Virdeforce, B. 1979, *A&AS*, 36, 317

Berdygina, S.V. 1993, *Astronomy Letters*, 19, 378

Berdygina, S.V., & Savanov, I.S., 1994, *Astronomy Letters*, 20, 755

Barstow, M.A., Bond, H.E., Burleigh, M.R., & Holberg, J.B. 2001, *MNRAS*, 322, 891

Bidelman, W.P., & Keenan, P.C. 1951, *ApJ*, 114, 473

Biemont, J., Palmeri, P., & Quinet, P. 2002, Database of rare earths at Mons University // <http://www.umh.ac.be/~astro/dream.html>

Boyarchuk, A., Antipova, L., Boyarchuk, M., & Savanov, I. 2001, *Astronomy reports*, 45, 301

Bruntt, H., Catala, C., Garrido, R., Rodriguez, E., Stutz, C., Knoglinger, P., Mittermayer, P., Bouret, J.C., Hua, T., Lignieres, F., Charpinet, S., Van't Veer-Menneret, C., & Ballereau, D. 2002, *A&A*, 389, 345

Burbidge, E.M., & Burbidge, G.R., 1957, *ApJ*, 126, 357

Burbidge, E.M., Burbidge, G.R., Fawler, W.A., & Hoyle, F. 1957, *Reviews Modern Physics*, 29, 547

Busso, M., Gallino, R., & Wasserburg, G. J. 1999, *ARA&A*, 37, 239

Cayrel de Strobel, G., Soubiran, C., Friel, E.D., Ralite, N., & Francois, P. 1997, *A&AS*, 124, 299

Chromey, F.R., Faber, S.M., Wood, A., & Danziger, I.J. 1969, *ApJ*, 158, 599

Cohen, J.C., Gratton, R.G., Behr, B.B., & Carreta, E. 1999, *ApJ*, 523, 739

Cowley C. 1995, *ASP Conf. Ser.*, 108, 170

Cowley, C.R., & Downs, P.L. 1980, *ApJ*, 236, 648

Cowley, C., Ryabchikova, T., Kupka, F., Bord, D., Mathys, G., & Bidelman, W. 2000, *MNRAS*, 317, 299

Delbouille, L., Roland, G., & Neven, L. 1973: Photometric Atlas of the Solar Spectrum from  $\lambda$  3000 to  $\lambda$  10000, Liege: Institut d'Astrophysique de l'Universite' de Liege.

de Medeiros, J.R., & Mayor, M. 1999, *A&AS*, 129, 433

Di Benedetto, G.P. 1998, *A&A*, 339, 858

Erspermer, D., & North, P. 2002, *A&A*, 383, 227

Fernandez-Villacanas J.L., Rego M., & Cornide M., 1990, *AJ*, 99, 1961

Galazutdinov, G.A. 1992, SAO RAS Preprint No.92

Gallino, R., Arlandini, C., Busso, M. et al. 1998, *ApJ*, 497, 388

Garreta, E., Cohen, J.G., Gratton, R.G., & Behr, B.B. 2001, *AJ*, 122, 1469

Girardi, L., Bressan, A., Bertelli, G., & Chiosi, C. 2000, *A&AS*, 141, 371

Gopka, V.F. & Yushchenko, A.V. 1995, *Astronomy Reports*, 39, 662

Gray, D.F., The observations and analysis of stellar photospheres, New York: Wiley, 1976

Gray, D.F. 1989, *ApJ*, 347, 1021

Gray, D.F., & Brown, K. 2001, *PASP*, 113, 723

Gratton, R.G. 1985, *A&A*, 148, 105

Gratton, L., Gaudenzi, S., Rossi, C., & Gratton, R.G., 1982, *MNRAS* 201, 807

Grevesse, N., & Sauval, A.J., 1998, *Space Science Reviews* 85, 161

Griffin, R.F. 1996, *The Observatory*, 116, 398

Griffin, R.F., & Keenan, P.C. 1992, *The Observatory*, 112, 168

Gurtovenko, E.A., & Kostik, R.I., 1989, *Fraunhofer spectr i sistema solnechnikh sil oscjaljatorov*. Kiev. Naukova Dumka. 198 p.

Holweger, H., & Muller, E.A. 1974, *Solar Physics*, 39, 19

Jorissen, A., Van Eck, S., Mayor, M., & Udry, S. 1998, *A&A* 332, 877

Keenan, P.C. & MacNeil, R.C. An Atlas of Spectra of the Collier Stars: Types G,K,M,S, and C, Ohio State Univ., 1976

Kovtyukh, V.V., & Gorlova, N.I. 2000, *A&A*, 358, 587

Kurucz, R.L. 1995, *ASP Conf. Ser.*, 81, 583

Leckrone, D.S., Proffitt, C.R., Wahlgren, G.M., Johansson, S.G., & Brage, T. 1999, *AJ*, 117, 1454

Liang, Y.C., Zhao, G., & Zhang, B., 2000, *A&A*, 363, 555

Liang, Y.C., Zhao, G., Chen, Y.Q., Qiu, H.M., & Zhang, B., 2003, *A&A*, 397, 257

Liu, J.H., Zhang, B., & Liang, Y.C. 2000, *A&A*, 363, 660

Malaney, R. 1987, *ApJ*, 321, 832

McClure, R.D., Fletcher, J.M., & Nemec, J.M. 1980, *ApJ*, 238, L35

McWilliam A., 1990, *ApJS*, 74, 1075

Morton, D.C. 2000, *ApJS*, 130, 403

Musaev, F., Galazutdinov, G., Sergeev, A., Karpov, N., & Pod'yachev, Y. 1999, *Kinematics and Physics of Selectial Bodies*, 15, 282

Pilachowski, C.A., 1977, *A&A*, 54, 465

Piskunov, N., Kupka, F., Ryabchikova, T., Weiss, W., & Jeffery, C. 1995, *A&AS*, 112, 525

Pourbaix, D., & Jorissen, A. 2000, *A&AS*, 145, 161

Rutten, R.J., & van der Zalm, E.B.J. *A&AS*, 1984, 55, 143

Sneden, C., Lambert, D., & Pilachowski, C., 1981, *ApJ*, 247, 1052

Sneden, C., Cowan, J.J., Ivans, I.I., Fuller, G.M., Burles, S., Beers, T.C., & Lawler, J.E., 2000, *ApJ*, 533, L139

Sneden, C., Cowan, J.J., Lawler J.E., Ivans I.I., Burles S., Beers, T., Primas, F., Hill, V., Truran, J.W., Fuller, G.M., Pfeiffer, B., & Kratz, K., 2003, *ApJ*, accepted for publication (*astro-ph/0303543*)

Straniero, O., Chieffi, A., Limongi, M., Busso, M., Gallino, R., & Arlandini, C. 1997, *ApJ*, 478, 332

Straniero, O., Gallino, R., Busso, M., Chieffi, A., Raiteri, C. M., Limongi, M., & Salaris, M. 1995, *ApJ*, 440, L85

Tarasova, T.N., 2002, *Astronomy Reports*, 46, 474

Tsymbal, V., & Cowley, C. 2000, private communication

Valenty, J.A., & Piskunov, N.E. 1996, *A&AS*, 118, 595

Walgren, G.M. 1996. *ASP Conf. Ser.*, 108, 240-253

Wallerstein, G., Iben, I., Parker, P., Boesgaard, A.M., Hale, G.M., Champagne, A.E., Barnes, C.A., Kappeler, F., Smith, V.V., Hoffman, R.D., Timmes, F.X., Sneden, C., Boyd, R.N., Meyer, B.S., & Lambert, D.L. 1997, *Reviews Modern Physics*, 69, 995

Yushchenko, A.V. 1998, Proc. of the 29th conf. of variable star research, Brno, Czech Republic, November 5-9, 201

Yushchenko, A.V., & Gopka, V.F. 1996a, *Astronomy Letters*, 22, 412

Yushchenko, A.V., & Gopka, V.F. 1996b, *Odessa Astron. Publ.*, 9, 86

Yushchenko, A.V., Gopka, V.F., Khokhlova, V.L., Musaev,  
F.A., & Bikmaev, I.F. 1999, Astronomy Letters, 25, 453  
Yushchenko, A., Gopka, V., Kim, C., Khokhlova, V., Shavrina,  
A., Musaev, F., Galazutdinov, G., Pavlenko, Y., Mishenina,  
T., Polosukhina, N., & North, P. 2002, Journal Korean  
Astron. Soc., 35, 209  
Zacs, L. 1994, A&A, 283, 937